NANO LETTERS

2009
Vol. 9, No. 9
3230-3233

Self-Supported Three-Dimensional Nanoelectrodes for Microbattery Applications

Seng Kian Cheah,[†] Emilie Perre,[†,‡] Mårten Rooth,[†] Mattis Fondell,[†] Anders Hårsta,[†] Leif Nyholm,[†] Mats Boman,[†] Torbjörn Gustafsson,[†] Jun Lu,[§] Patrice Simon,[‡] and Kristina Edström*[,†]

Department of Materials Chemistry, The Ångström Laboratory, Uppsala University, Box 538, SE-751 21 Uppsala, Sweden, Université de Toulouse, CIRIMAT UMR CNRS 5085, 118 rte de Narbonne, 31062 Toulouse Cedex 9, France, and Department of Engineering Sciences, The Ångström Laboratory, Uppsala University, Box 534, SE-751 21 Uppsala, Sweden

Received May 10, 2009; Revised Manuscript Received June 3, 2009

ABSTRACT

A nanostructured three-dimensional (3D) microbattery has been produced and cycled in a Li-ion battery. It consists of a current collector of aluminum nanorods, a uniform layer of 17 nm TiO_2 covering the nanorods made using ALD, an electrolyte and metallic lithium counter electrode. The battery is electrochemically cycled more than 50 times. The increase in total capacity is 10 times when using a 3D architechture compared to a 2D system for the same footprint area.

Li-ion batteries are today used for a wide range of applications such as portable electronics, medical devices, and in prototypes for hybrid electric vehicles (HEV). The chemistry in the battery can be tuned depending on the performance requirement for the different applications and hence the chemical content of an HEV battery is not in detail the same as for a mobile phone battery. This tuning allows for a miniaturization to make small scale power supplies and energy storage devices. However, to make a high energy and power unit on a small footprint area (for example <1 cm^2) requires the use of nanostructured architectures, three-dimensional (3D) microbatteries. Three-dimensional microbatteries can be used in powering, for instance, MEMS-based sensors and actuators,[1] biosensors, and other similar applications. There are still only a few examples in literature of 3D microbatteries.[2−4] In this work, we show for the first time how a 3D Li-ion battery can be made based on a nanostructured current collector of aluminum in the form of aluminum nanorods, and that it is possible to uniformly deposit a cathode material (in this case TiO_2) on the rods despite the narrow distance between them (∼20 nm for homemade membranes and a minimum 50 nm for commercial membranes) and then to cycle it in a Li-ion battery. We selected TiO_2 based on its simplicity to synthesize thin films with the anatase structure with a broad selection of different techniques. Anatase can host up to 0.5 Li per formula unit and with TiO_2 particles <40 nm up to 0.8 Li can be stored.[5] TiO_2 is also abundant, nontoxic, and cheap.

We have earlier shown that we can grow aluminum nanorods using a direct electrodeposition procedure into a nanoporous alumina membrane used as a template.[6] The rods can be synthesized in both commercial nanoporous membranes (Anodisc 47, Whatman) (Figure 1a,b) and in membranes synthesized in-house through either mild- or hard anodization as described in literature.[7,8] Our results presented here are based on commercial membranes. All the steps for the preparation of aluminum nanorods were carried out in an argon-filled glovebox (O_2 and H_2O <2 ppm) since the ionic liquid, 1-ethyl-3-methylimidazolium chloride ([EMIm]-Cl)/aluminum chloride ($AlCl_3$) (1:2 ratio), used as the deposition electrolyte can easily decompose in contact with water.

The acidic electrolyte was prepared by slow addition of aluminum chloride (anhydrous powder, 99.99%, Sigma-Aldrich) into 1-ethyl-3-methylimidazolium chloride (98.5%, Fluka) under continuous stirring. Since the reaction of $AlCl_3$ with [EMIm]Cl is highly exothermic, a light white smoke could be observed if the addition of the $AlCl_3$ was too fast. Therefore, care must be taken to prevent the decomposition of the electrolyte. A brownish liquid was formed at the end of the mixing.

* To whom correspondence should be addressed. E-mail: Kristina.edstrom@mkem.uu.se. Tel: +46-18-4713713. Fax: +46-18-513548.
[†] Department of Materials Chemistry, Uppsala University.
[‡] Université de Toulouse.
[§] Department of Engineering Sciences, Uppsala University.

10.1021/nl9014843 CCC: $40.75
Published on Web 07/02/2009

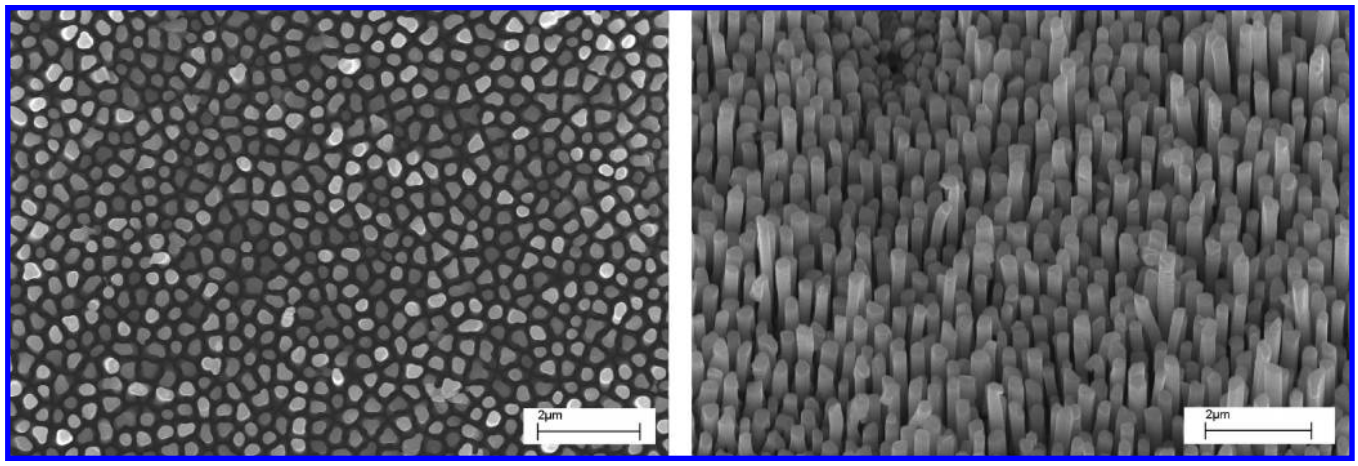

Figure 1. SEM image of aluminum nanorods synthesized by −0.4 V vs Al pulses for 50 ms and −0.1 V vs Al pulses for 200 ms 14 400 times in a commercial membrane top view (left) and side/tilted view (right).

To prepare the aluminum nanorods, a three-electrode setup connected to a potentiostat/galvanostat Autolab PGSTAT30 was used for the voltage pulse electrodeposition.[6] Two 1 cm × 1 cm aluminum plates were used as the working and counter electrodes. A thick glass fiber separator was filled with the electrolyte. The reference electrode was an aluminum wire with 1 mm diameter (99.999%, Goodfellow) immersed in the electrolyte ([[EMIm]Cl/$AlCl_3$, molar ratio 1:2). The free-standing aluminum nanorods were then obtained by dissolving the alumina template outside the glovebox in an aqueous solution of CrO_3 (1.8 wt %) and H_3PO_4 (6 wt %)[9] followed by rinsing in water.

The aluminum nanorods, however, do not grow as evenly as the Cu nanorods reported by Taberna et al.[10] There is instead an "island-like" growth resulting in an uneven height-distribution. This can depend on nucleation problems on the flat substrate or of the nonhomogenous distribution of pores in the commercial nanoporous aluminum membrane. The best nanorods, however, were obtained when applying a pulse potential deposition sequence, −0.4 V versus Al for 50 ms then −0.1 V versus Al for 200 ms.

The electrode material TiO_2 was then deposited on to the aluminum nanorods by the use of atomic layer deposition (ALD). ALD is a method that can meet the high demands of controlled thickness and high uniformity on nonplanar substrates.[11] ALD is therefore an ideal method for depositing TiO_2 on aluminum nanorods and in the present study TiO_2 was deposited from TiI_4 and H_2O (see, e.g., ref 12). An Al substrate covered with aluminum nanorods was placed on a substrate holder in the ALD reactor. The evaporation zone and the deposition zone were preheated to 100 and 200 °C, respectively, for half an hour. The deposition temperature was 200 °C and the TiI_4 was evaporated at 108 °C. These temperatures were maintained through out the rest of the experiment.

The ALD process contained four different pulses in which each lasted for 15 s. In the first pulse, TiI_4 was evaporated and carried to the deposition zone by inert nitrogen gas where it reacted with the surface of the substrate. As TiI_4 adsorbed on the surface, one or more of the ligands were broken off and entered the gas phase in form of I or I_2 depending on the temperature. The second pulse was a purging pulse where the reaction chamber was flushed with N_2 to remove reaction biproducts (I, I_2) and the excess of TiI_4. The third pulse was the water pulse where water vapor reacted with the adsorbed titanium iodide forming TiO_2 and HI. The fourth and last pulse was another purging pulse in which the HI and excess water vapor was removed by a N_2 pulse. These four pulses formed a cycle. One hundred and fifty cycles were used for the deposition of TiO_2.

X-ray diffraction characterization was then carried out on the deposited film using a Siemens D5000 grazing incidence diffractometer and Cu Kα radiation at 1° grazing angle. The TiO_2 film showed to have an anatase structure.

The Al nanorods with the deposited anatase were further examined with HRTEM (see Figure 2). The HRTEM (Tecnai F30 ST, FEI) was used to determine the thickness and crystalline phases of the film. It was shown that a 17 nm thick layer of TiO_2 was deposited onto the rods. In Figure 2a, the HRTEM micrograph shows that the whole surface of the Al nanorods is covered by a conformal layer of TiO_2 deposited by ALD; even the edges are covered with TiO_2. In Figure 2b, the narrow spacing between nanorods, around 40 nm, is also covered by the conformal layer of TiO_2. In Figure 2c, a thin layer of Al_2O_3, approximately 4 nm, can be observed in between the TiO_2 layer and the Al nanorods. The oxide layer forms due to the exposure to air before the deposition of TiO_2. This oxide layer not only provides extra protection to the Al nanorods from reactions with the electrolyte in a battery but also facilitates the growth and adhesion of the TiO_2 layer on the rods. The HRTEM study also shows the structure to be more complicated than seen from the X-ray diffraction experiment only. The combination of the techniques shows the deposited TiO_2 film to consist of amorphous matrix with nanocrystalline anatase.

The electrode was then tested in a Li-ion battery context. Galvanostatic cycling tests were performed using the TiO_2 on the aluminum nanorods as the working electrode, lithium metal as a counter electrode, and a glass fiber separator soaked with an electrolyte of 1 M $LiClO_4$−PC (propylene

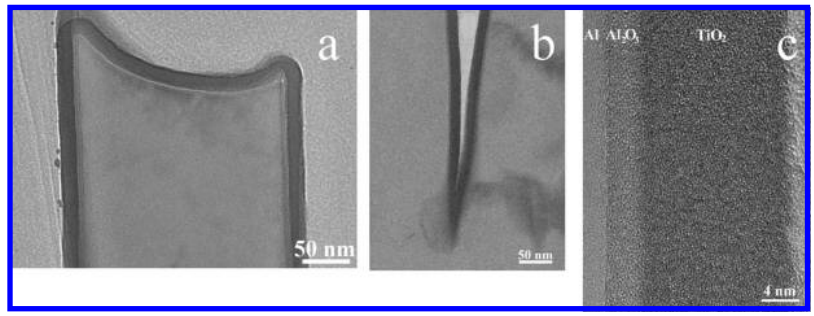

Figure 2. HRTEM images of Al nanorods with deposited TiO_2 at 200 °C for 150 cycles. A homogeneous TiO_2 layer (dark color) is covering the whole surface of the nanorod tip (a). The TiO_2 layer is also covering the narrow spacing in between the nanorods (b). There is a 4 nm thick Al_2O_3 layer between the TiO_2 layer and the nanorod (c).

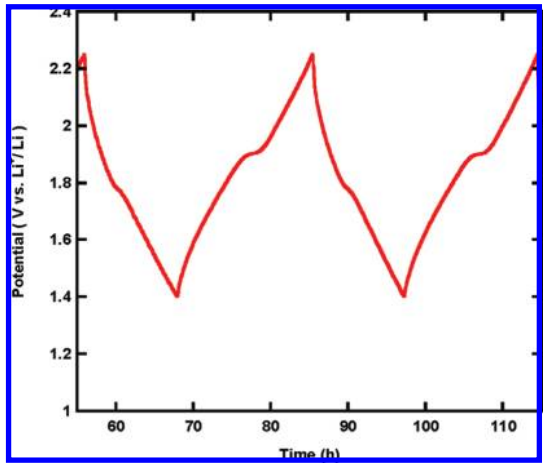

Figure 3. Cycles 3 and 4 in the galvanostatic charge−discharge curve of TiO_2 deposited on the Al nanostructured current collector. Cycled at 1 μA.

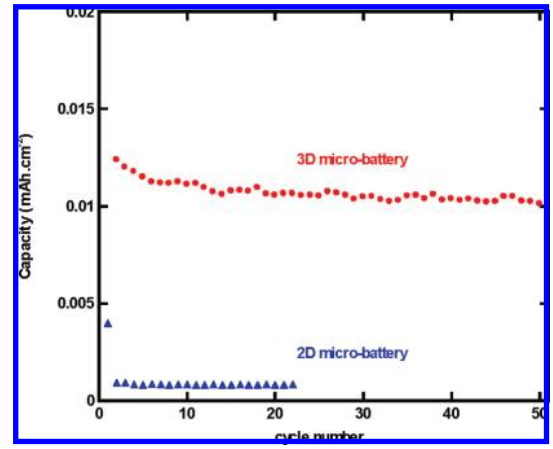

Figure 4. Normalized capacity (mAh/cm^2 of geometrical surface area) for the 3D microbattery with TiO_2 deposited on an Al nanorod current collector and the 2D electrode with TiO_2 deposited on a flat Al plate. The galvanostatic cycling current is 0.001 mA.

carbonate) (the salt was dried at 80 °C overnight and the PC from Merck was used as received). The water content is <10 ppm (Karl Fischer titration). The electrochemical cycling tests were carried out with a Digatron battery testing system between 3.0 and 1.4 V. Cells were assembled in a glovebox under argon atmosphere (<2 ppm H_2O and O_2) and packed into a polymer-coated aluminum pouch.

The galvanostatic charge−discharge curve of TiO_2 deposited on the nanostructured current collector is presented in Figure 3. The curve shows the typical behavior of a semicrystalline sample. The plateaus observed at 1.77 V during discharge and at 1.9 V when charging, correspond to the insertion/extraction of lithium within the crystalline part of TiO_2.

To be able to compare the cycling results for the 2D and 3D architectures, the amount of deposited TiO_2 needs to be determined. Considering for both 2D and 3D substrates, a TiO_2 layer of 17 nm and a density of 3.895 g·cm^{-3}, the mass of deposited TiO_2 can be calculated. For a 1 cm^2 × 1 cm^2 flat Al substrate, the mass deposited is equal to 0.0066 mg, while for an Al substrate containing nanorods onto a footprint area of 1 cm^2 × 1 cm^2 the mass deposited is equal to 0.0667 mg. The amount of TiO_2 deposited onto the 3D substrate has been evaluated based on the calculation of area gain reported by Perre et al.[6] Assuming a constant nanorod diameter of 200 nm, an average height of 2 μm, and an interpore distance of 400 nm, the area gain is equal to 10.07.

The theoretical capacity of TiO_2 is 167.7 mAh·g^{-1} for 0.5 inserted Li-ion, thus corresponding to theoretical capacity values of 0.0011 mAh·cm^{-2} for the 2D microbattery and 0.0112 mAh·cm^{-2} for the 3D microbattery.

As expected the results of the battery cycling show an increase in total capacity when using a 3D architectured electrode compared to a 2D electrode (see Figure 5) due to the higher amount of TiO_2 deposited onto the 3D nanostructured current collector. This increase in capacity by a factor of 10 is consistent with the calculated area gained on a 3D substrate compared to a 2D substrate.

For both the 3D and the 2D electrodes, the measured capacity values are close to the theoretical values and are maintenained upon cycling. Thus showing that due to the small thickness deposited, TiO_2 accommodates easily the structural changes taking place during the insertion of 0.5 Li ion. This result is consistent with the reported result by Sudant et al.[13] The good correlation between the calculated and measured capacity values also confirms the efficiency of the ALD process when a conformal layer needs to be deposited onto a complex 3D substrate.

The rate capability of the nanostructured TiO_2 electrode was also tested and shown to be excellent. This is shown in

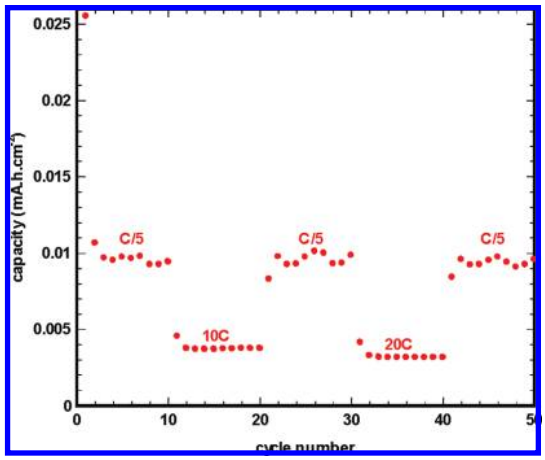

Figure 5. Capacity per footprint area of a nanostructured cell that has been cycled between 3.0 and 1 V. The cycling rate has been varied upon cycling to evaluate its rate capability.

Figure 5, where TiO_2 was cycled at different rates and still retained its initial capacity values after 50 cycles. The high irreversible capacity observed in the first cycle can be attributed to the presence of defects within the TiO_2 amorphous structure that trap the Li^+ ions.[4]

All these results show the 3D nanostructured electrode to be a promising system. The electrodes are able to provide approximately 40 and 35% of the initial capacity (cycling at C/5 rate) even though the cycling current has been increased by 50 (10 C) and 100 (20 C) times, respectively. The outstanding performance is the result of the nanostructured active material and the conformal deposition. Despite of the small grain size and short diffusion length, the electrode still shows the typical intercalation behavior for a crystalline TiO_2. In a previous report,[5] the biphasic property of the TiO_2 during charge and discharge started to disappear when the size of the TiO_2 is smaller than 120 nm.

The results revealed in this study are promising for the future development of 3D nanostructured architectures for lithium-based microbatteries. The arrays of aluminum current collector coated by TiO_2 showed higher volumetric capacity as compared to the results reported by Min et al.[2] and higher rate capability compared to the design proposed by Golodnistky et al.[3]

Ortiz et al.[4] recently reported the cycling data of dense arrays of TiO_2 anatase nanotubes grown by anodization of a Ti substrate. They presented high capacity values per footprint area. However, in such architectures power performances are driven by the height of the active material pillars;[1] accordingly power capability was limited to 2C.

Our study opens new paths for the study of deposition processes of other cathode materials than TiO_2 on complicated nanostructured current collectors.

Acknowledgment. This work is supported by the Swedish Research Council (VR), ALISTORE-ERI within EU-FP6 framework, and SUPERLION within EU-FP7. We also acknowledge the EUROPEAN ERASMUS MUNDUS PROGRAM from the European commission and the French Ministry of Research for, respectively, the Erasmus Mundus Grant of S.K.C. and the Ph.D. Grant of E.P.

References

(1) Long, J. W.; Dunn, B.; Rolison, D. R.; White, H. S. *Chem. Rev.* **2004**, *104* (10), 4463–4492.
(2) Min, H.-S.; Park, B. Y.; Taherabadi, L.; Wang, C.; Yeh, Y.; Zaouk, R.; Madou, M. R.; Dunn, B. *J. Power Sources* **2008**, *178*, 795–800.
(3) Golodnitsky, D.; Nathan, M.; Yufit, V.; Strauss, E.; Freedman, K.; Burstein, L.; Gladkich, A.; Peled, E. *Solid State Ionics* **2006**, *177*, 2811–2819.
(4) Ortiz, G. F.; Hanzu, I.; Djenizian, T.; Lavela, P.; Tirado, J. L.; Knauth, P. *Chem. Mater.* **2009**, *21*, 63–67.
(5) Wagemaker, M.; Borghols, W. J. H.; Mulder, F. M. *J. Am. Chem. Soc.* **2007**, *129* (14), 4323–4327.
(6) Perre, E.; Nyholm, l.; Gustafsson, T.; Taberna, P.-L.; Simon, P.; Edström, K. *Electrochem. Commun.* **2008**, *10* (10), 1467–1470.
(7) Li, A. P.; Müller, F.; Birner, A.; Nielsch, K.; Gösele, U. *J. Appl. Phys.* **1998**, *84* (11), 6023–6026.
(8) Lee, W.; Ji, R.; Gösele, U.; Nielsch, K. *Nat. Mater.* **2006**, *5*, 741–747.
(9) Masuda, H.; Satoh, M. *Jpn. J. Appl. Phys.* **1996**, *35* (1B), L126−L129.
(10) Taberna, P.-L.; Mitra, S.; Poizot, P.; Simon, P.; Tarascon, J.-M. *Nat. Mater.* **2006**, *5*, 567–573.
(11) Knez, M.; Nielsch, K.; Niinistö, L. *Adv. Mater.* **2007**, *19* (21), 3425–3438.
(12) Rooth, M.; Quinlan, R. A.; Widenkvist, E.; Lu, J.; Grennberg, H.; Holloway, B. B.; Hårsta, A.; Jansson, U. *J. Cryst. Growth* **2009**, *311* (2), 373–377.
(13) Sudant, G.; Baudrin, E.; Larcher, D.; Tarascon, J.-M. *J. Mater. Chem.* **2005**, *15*, 1263–1269.

NL9014843